RSC Advances

PAPER

View Article Online
View Journal | View Issue

Cite this: *RSC Adv.*, 2017, **7**, 17489

Visible-light-activated photoelectrochemical biosensor for the detection of the pesticide acetochlor in vegetables and fruit based on its inhibition of glucose oxidase†

Dangqin Jin,* Aiqin Gong and Hui Zhou

A new and sensitive photoelectrochemical (PEC) biosensor which is visible-light-activated was fabricated based on acetochlor's ability to inhibit glucose oxidase (GOx) activity. An NH_2-MIL-125(Ti)/TiO_2 nanocomposite, as a new functional material, was used for the immobilization of GOx by using chitosan (CS) as the dispersion matrix. Under visible light irradiation, the GOx/CS/NH_2-MIL-125(Ti)/TiO_2 nanocomposite can generate a stable photocurrent in a glucose solution. When acetochlor was added to a phosphate buffer solution containing glucose, the activity of GOx was inhibited thus causing a photocurrent drop, and the photocurrent was inversely proportional to the acetochlor concentration. A corresponding analytical method was developed. The inhibition of the photocurrent was proportional to the concentration of acetochlor in the range from 0.02 to 1.0 nM and in the range from 10 to 200 nM with a detection limit of 0.003 nM (S/N = 3). The study is a successful attempt to make a PEC biosensor based on monitoring the activity and inhibition of GOx, and shows its practical application in acetochlor detection in fruit and vegetable samples.

Received 5th January 2017
Accepted 28th February 2017

DOI: 10.1039/c7ra00164a

rsc.li/rsc-advances

1. Introduction

Acetochlor (2-chloro-*N*-(ethoxymethyl)-*N*-(2-ethyl-6-methylphenyl)-acetamide), as one of the most important herbicides in the world, has been widely used as a pesticide in agriculture for weed control. However, acetochlor use has defined limits in many countries[1] because it has been classified by the US Environmental Protection Agency (USEPA) as a B-2 carcinogen.[2] The registration for acetochlor states that concentrations of acetochlor should not exceed 0.37 nM in groundwater or 7.41 nM as an annual average in surface water.[2] Long-term exposure to herbicides may cause imbalances in reactive oxygen species that could ultimately harm plant and food quality.[3] In order to protect human health and environmental safety, the detection of acetochlor residue is becoming increasingly important. In the past decades, well established methods have included gas chromatography (GC), high performance liquid chromatography (HPLC), gas chromatography-mass spectrometry (GC-MS), liquid chromatography-mass spectrometry (LC-MS),[4,5] and immunosorbent assays.[6] Despite many advances in acetochlor detection, sensitive, selective, stable and facile methods still need to be explored.

Photoelectrochemical (PEC) sensors have attracted the attention of researchers as a newly developed and sensitive analytical technique for targeted molecules and ions.[7,8] Compared with electrochemical detection, PEC sensors have very low backgrounds owing to the separation of the excitation source (light) and detection signal (photocurrent). Meanwhile, PEC sensors have some of the advantages of electrochemical sensors, such as low background signals, high sensitivity, inherent miniaturization, portability and easy automation.[9] However, photocatalytic oxidation lacks selectivity due to the nature of the hydroxyl radicals or holes generated in photocatalytic oxidation, and it is not suitable for selective analysis.[10] Therefore, how to achieve selectivity in a photoelectrochemical sensor is a quite critical issue. A photoelectrochemical biosensor based on the inhibition of different enzymes known to recognise the target molecule has been proposed and has developed rapidly.[11] Recently, photoelectrochemical sensors based on enzyme inhibition have been fabricated, and exhibited favorable selectivity towards target molecules and ions.[12,13] Glucose oxidase (GOx) is often used as an enzyme in studies of inhibition due to its low cost, good stability and high specific activity. However, most of the GOx based photoelectrochemical biosensors in the literature have been developed for the determination of the substrates of GOx.[14] There are only a few works reporting the inhibition of immobilized GOx using an electrochemical method,[12,13] and none on the photoelectrochemical detection of acetochlor based on GOx activity inhibition.

Department of Chemical Engineering, Yangzhou Polytechnic Institute, Yangzhou 225127, P. R. China. E-mail: jindangqin@163.com; Fax: +86 514 87433017; Tel: +86 514 87433053

† Electronic supplementary information (ESI) available. See DOI: 10.1039/c7ra00164a

Currently, the exploration of photoactive materials based sensing platforms is a critical issue because the material choices are directly related to the stability of the biological recognition element and the final sensing performance. Typically, TiO_2-based composites have proved to be excellent electrode materials in PEC sensors owing to their good biocompatibility, relative conductivity, inexpensiveness, environmental safety, and chemical and thermal stability.[15] Many efforts have been made toward the development of TiO_2-based composites for visible-light-activated photoelectrochemical biosensing, which could greatly increase the efficient utilization of solar light and reduce the destructive effects of UV light and the photogenerated holes from the illuminated TiO_2 on the biomolecules.[15,16]

NH_2-MIL-125(Ti) (MIL stands for Materials from Institute Lavoisier), a robust amino-functionalized titanium(IV) based metal–organic framework (MOF)[17] with the formula $Ti_8O_8(OH)_4(NH_2\text{-BDC})_6$, has attractive redox and photocatalytic properties.[18] The inclusion of amine moieties slightly extends the light absorption of MIL-125(Ti) to the visible region. These characteristics make NH_2-MIL-125(Ti) a promising modifier in photocatalysis and extend the scope of applications for photoelectrochemical sensors.[19,20] The coupling of small band gap semiconductors with large band gap ones to facilitate charge separation is an efficient way to improve photocurrents.[21,22] Recently, our group developed a simple solvothermal method to fabricate NH_2-MIL-125(Ti)/TiO_2 nanocomposite arrays and further explored its applications in photoelectrochemical sensors.[23] NH_2-MIL-125(Ti)/TiO_2 with a large surface area should be a good immobilization matrix for biomolecules. Chitosan (CS), a natural biopolymer with unique structural features, is commonly used to disperse nanomaterials and immobilize enzymes for constructing biosensors due to its excellent film forming ability, nontoxicity, biocompatibility, mechanical strength, and good water permeability.[24,25] Inspired by this idea, here we present for the first time novel applications of CS/NH_2-MIL-125(Ti)/TiO_2 for the PEC biosensing of acetochlor under visible light irradiation.

The first application of CS/NH_2-MIL-125(Ti)/TiO_2 with the biomolecule glucose oxidase (GOx) yields a novel GOx/CS/NH_2-MIL-125(Ti)/TiO_2 hybrid as a photoelectrochemical biosensing platform. Scheme 1 illustrates the construction and operation process of the biosensor. GOx can catalyze glucose to produce H_2O_2, which acts as an electron donor for the photogenerated holes in the valence band of the NH_2-MIL-125(Ti)/TiO_2 and thus enhances the photocurrent upon visible light irradiation.[26] However, the enhanced photocurrent will obviously be decreased when the enzyme activity is inhibited by acetochlor. The percentage GOx activity inhibition was used for the quantitative detection of acetochlor. The new approach greatly reduces the destructive effects of UV light and the photogenerated holes from the illuminated TiO_2 on the biomolecules, *via* constructing a novel biofunctional GOx/CS/NH_2-MIL-125(Ti)/TiO_2 photoactive sensing platform. This methodology not only overcame the selectivity shortcomings of our previously developed photoelectrochemical sensors for acetochlor,[27] but also opened up a new type of photoelectrode for photoelectrochemical sensing. To our knowledge, no data have been found concerning utilizing GOx/CS/NH_2-MIL-125(Ti)/TiO_2 for the photoelectrochemical biosensing of acetochlor. It is expected that such a nanostructured composite GOx/CS/NH_2-MIL-125(Ti)/TiO_2 would considerably facilitate the sensitive determination of acetochlor.

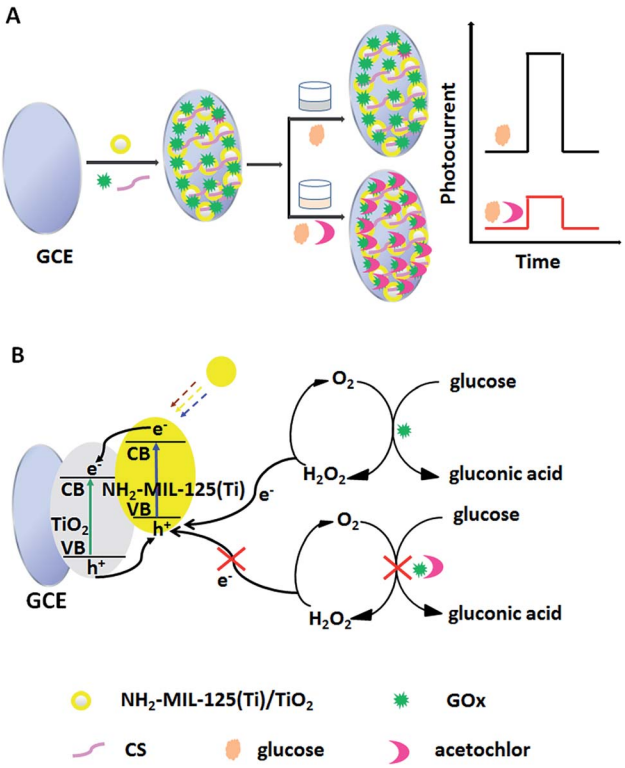

Scheme 1 (A) Fabrication process of the GOx/CS/NH_2-MIL-125(Ti)/TiO_2 biosensor and (B) the corresponding electron-transfer mechanism.

2. Experimental section

2.1. Reagents

Glucose oxidase (GOx) (EC 1.1.3.4, 109 U mg^{-1}, type VII from *Aspergillus niger*) was obtained from Amresco Chemical Co., Ltd. Acetochlor, TiO_2 nanopowder (anatase, <25 nm, 99.7%), chitosan (CS), D-(+)-glucose, 2-aminoterephthalic acid ($H_2BDC\text{-}NH_2$), tetrabutyl titanate (TBT), *N*,*N*-dimethylformamide (DMF), and methanol were purchased from Sinopharm Chemical Reagent Co., Ltd (Shanghai, China). A phosphate buffer was prepared by mixing stock solutions of 0.1 M NaH_2PO_4 and 0.1 M Na_2HPO_4, and then adjusting the pH with H_3PO_4 or NaOH. A glucose stock solution was prepared with 0.1 M pH 7.0 phosphate buffer and was allowed to mutarotate at room temperature overnight before use. All the other chemicals were of analytical grade and were used as received without any purification process. Deionized double-distilled water (18.6 MΩ) (Millipore Co. Ltd.) was used to prepare all the solutions, and the pH value of the phosphate buffer was 7.0 unless indicated otherwise.

2.2. Apparatus

A Hitachi S-4800 scanning electron microscope (Hitachi, Tokyo, Japan) using an acceleration voltage of 15 kV was used to obtain scanning electron microscopy (SEM) images. Diffuse reflectance UV/Vis spectra were recorded using a Perkin-Elmer Lambda 900 spectrophotometer in the 200–700 nm range. Fourier-transform infrared (FTIR) spectra were recorded on a Nicolet iS10 instrument (Nicolet, USA). The photoelectrochemical experiments were performed on a CHI760D electrochemical analyzer (Chenhua Instrument Corporation, Shanghai, China) with an in-house-built PEC system, where a 250 W halogen lamp acted as the irradiation source (λ > 400 nm). A conventional three electrode system was used comprising a bare or modified glassy carbon electrode (GCE) (3 mm in diameter, Shanghai Chenhua, China) as the working electrode, a platinum wire as the auxiliary electrode and a saturated calomel electrode (SCE) as the reference electrode. All the photocurrent measurements were carried out by the amperometric current–time curve technique upon visible light irradiation (λ > 400 nm) at a constant potential of 0.2 V in a phosphate buffer solution (pH 7.0, 0.1 M) containing glucose (0.6 mM) at room temperature (25 ± 2 °C).

2.3. Preparation of NH_2-MIL-125(Ti)/TiO_2 and different electrodes

NH_2-MIL-125(Ti)/TiO_2 was obtained according to the literature method with a little modification.[23,28] First, tetrabutyl titanate (TBT), 2-aminoterephthalic acid (H_2BDC-NH_2), TiO_2 nanopowder, *N*,*N*-dimethylformamide (DMF), and methanol were mixed together in the ratio 1.0 mmol : 3 mmol : 6 mmol : 12.5 mL : 1.5 mL. Then the suspension was carefully transferred into a Teflon lined autoclave, and heated at 150 °C for 20 h. After the suspension was allowed to cool to room temperature, it was filtered and washed thrice with DMF and methanol to obtain a pale yellow powder product. Finally, the solid product was dried under vacuum at 60 °C for 6 h to get the final NH_2-MIL-125(Ti)/TiO_2 photocatalyst.

Chitosan, a natural biopolymer with good biocompatibility and excellent film forming ability,[24,25] was used to help the stable dispersion of NH_2-MIL-125(Ti)/TiO_2 in aqueous solution. A chitosan solution (0.5%) (w/v) was prepared by dissolving 0.5 g chitosan powder in 100.0 mL of 1.0% acetic acid solution. 1.0 mg of NH_2-MIL-125(Ti)/TiO_2 was dispersed in 0.5% chitosan solution with ultrasonication for 30 min, followed by the addition of 10.0 mg GOx, with gentle mixing for 15 min. The GCE was polished with 0.3 μm of Al_2O_3, washed with ethanol and distilled water and dried in air. 10 μL of the above GOx/CS/NH_2-MIL-125(Ti)/TiO_2 suspension was coated onto the clean GCE and dried at 4 °C to obtain a GOx/CS/NH_2-MIL-125(Ti)/TiO_2-modified GCE. The resulting electrode was marked as GOx/CS/NH_2-MIL-125(Ti)/TiO_2/GCE. When they were not in use, the enzyme electrodes were stored at 4 °C in a refrigerator. For comparison, a TiO_2 modified GCE and an NH_2-MIL-125(Ti)/TiO_2 modified GCE were prepared similarly.

2.4. Photoelectrochemical biosensing under visible light illumination

For the determination of acetochlor, the obtained GOx/CS/NH_2-MIL-125(Ti)/TiO_2/GCE electrode was immersed in phosphate buffers (0.1 M, pH 7.0) containing different concentrations of acetochlor at room temperature for 10 min, and the electrode was transferred to a glass cell containing 10.0 mL (0.1 M, pH 7.0) phosphate buffer containing 0.6 mM glucose, this being the enzyme substrate concentration, to study the PEC response. For comparison, PEC responses were also measured by the same procedure except that the GOx/CS/NH_2-MIL-125(Ti)/TiO_2/GCE electrode was immersed in a phosphate buffer without acetochlor for 10 min. The inhibition by acetochlor was calculated as follows:

$$\text{Inhibition } (\%) = \frac{I_{\text{without}} - I_{\text{with}}}{I_{\text{without}}} \times 100$$

where I_{without} is the photocurrent response to glucose in the absence of acetochlor and I_{with} is the photocurrent response in the presence of acetochlor.

After each inhibition, the working electrode was soaked in phosphate buffer (pH 7.0) to be reactivated, for 5 min.

2.5. Sample preparation

To demonstrate the feasibility of the proposed method, we applied it to the determination of acetochlor in fruit and vegetable samples. 50 g of commercially available fruits and vegetables (strawberries, greens, tomatoes and cucumbers) were chopped into small pieces to obtain thoroughly mixed homogenates. A 5 g portion of each of the samples was uniformly sprayed with a known amount of the acetochlor stock solution. The samples were placed in a glass disk for 12 h. The contaminated samples were taken out and washed with water three times, placed in a centrifuge tube with the addition of 10.0 mL of methyl cyanide, shaken vigorously for 2 min, and then centrifuged at 3000 rpm for 10 min. Before the recovery studies, the samples were tested by the GC-MS method to prove them to be free from acetochlor.

3. Results and discussion

3.1. Characterizations of NH_2-MIL-125(Ti)/TiO_2, NH_2-MIL-125(Ti)/TiO_2/CS, and GOx/CS/NH_2-MIL-125(Ti)/TiO_2

Fig. 1A shows the structure of the synthesized NH_2-MIL-125(Ti)/TiO_2. The sheet morphology of NH_2-MIL-125(Ti)/TiO_2 can be clearly observed. Fig. 1B shows an SEM image of the NH_2-MIL-125(Ti)/TiO_2 which was dispersed in a chitosan (CS) solution. A more uniform structure for NH_2-MIL-125(Ti)/TiO_2 was obtained in the presence of CS, indicating that CS was a good dispersing agent for NH_2-MIL-125(Ti)/TiO_2. Chitosan, a natural linear polyaminosaccharide, has a hydrophilic/hydrophobic nature, which makes it suitable for improving the solubility of NH_2-MIL-125(Ti)/TiO_2 in aqueous solution.[29] Its linear polyglucosamine chains have a strong tendency to adsorb on the NH_2-MIL-125(Ti)/TiO_2 sheets *via* van der Waals forces and hydrophobic interactions, and the hydrophilic amino and hydroxyl groups

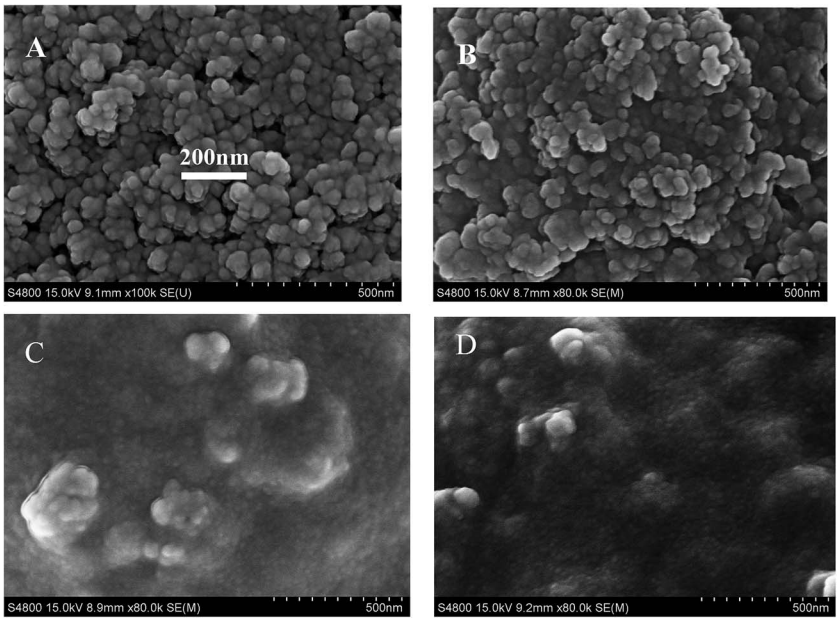

Fig. 1 (A) SEM image of NH_2-MIL-125(Ti)/TiO_2 dispersed in aqueous solution; (B) SEM image of NH_2-MIL-125(Ti)/TiO_2 dispersed in 0.5% (w/v) chitosan solution; (C) SEM image of GOx immobilized in NH_2-MIL-125(Ti)/TiO_2 which was dispersed in water (GOx/NH_2-MIL-125(Ti)/TiO_2); (D) SEM image of GOx immobilized in NH_2-MIL-125(Ti)/TiO_2 which was dispersed in chitosan solution (GOx/CS NH_2-MIL-125(Ti)/TiO_2).

help to disperse the functionalized NH_2-MIL-125(Ti)/TiO_2 in water solution. After GOx molecules were trapped in the NH_2-MIL-125(Ti)/TiO_2/CS composite, its SEM image (Fig. 1D) exhibited a more obviously continuous and uniform surface morphology than GOx trapped in the NH_2-MIL-125(Ti)/TiO_2 composite in the absence of CS (Fig. 1C), suggesting the successful immobilization of GOx in the NH_2-MIL-125(Ti)/TiO_2/CS nanocomposite film.

Fig. S1† shows the absorption spectra of GOx, NH_2-MIL-125(Ti)/TiO_2, GOx/NH_2-MIL-125(Ti)/TiO_2 and GOx/CS/NH_2-MIL-125(Ti)/TiO_2. Pure GOx had absorption in the visible region with maximum values at 382 and 453 nm (curve a), which were consistent with a previous report.[30] NH_2-MIL-125(Ti)/TiO_2 nanocomposites had their own strong absorption at 389 nm (curve b). For GOx/NH_2-MIL-125(Ti)/TiO_2 (curve c), the absorption value at 453 nm remained stable, while the absorption value at 385 nm shifted between 382 and 389 nm, which might be due to the interaction between the GOx and the NH_2-MIL-125(Ti)/TiO_2 nanocomposites.[30] The absorption value for GOx/CS/NH_2-MIL-125(Ti)/TiO_2 (curve d) is basically the same as that of GOx/NH_2-MIL-125(Ti)/TiO_2 (curve c). These results indicated that GOx was firmly immobilized on the NH_2-MIL-125(Ti)/TiO_2 nanocomposites.

Fig. S2† shows FTIR spectra of NH_2-MIL-125(Ti)/TiO_2 (a), GOx (b), GOx/NH_2-MIL-125(Ti)/TiO_2 (c), and GOx/CS/NH_2-MIL-125(Ti)/TiO_2 (d). The signal for NH_2-MIL-125(Ti)/TiO_2 at 400–800 cm^{-1} is characteristic of O–Ti–O,[31] a large, broad band centered at 3361 cm^{-1} was assigned to symmetric and asymmetric stretching vibrations of primary amines,[32] and the two obvious peaks at 1537 and 1432 cm^{-1} corresponded with the carboxylate linker.[31] For GOx, the infrared peaks of amide I and amide II with center positions at 1651 cm^{-1} and 1549 cm^{-1} could be observed, which were generally used as an indication of protein denaturation and conformational change upon immobilization.[33] The typical amide I and amide II adsorption peaks could also be observed for the GOx/NH_2-MIL-125(Ti)/TiO_2 and GOx/CS/NH_2-MIL-125(Ti)/TiO_2 samples, which suggested that the GOx retained its essential features after being adsorbed on the surfaces of NH_2-MIL-125(Ti)/TiO_2 and GOx/CS/NH_2-MIL-125(Ti)/TiO_2, and revealed the good biocompatibility of NH_2-MIL-125(Ti)/TiO_2. The amide adsorption peaks had a red shift to 1669 cm^{-1} and 1559 cm^{-1}, which might be due to the strong electrostatic interaction between the anchored GOx and NH_2-MIL-125(Ti)/TiO_2.[14]

The UV-vis diffuse reflection spectra were used to demonstrate the absorption edges of the fabricated electrodes, including TiO_2, NH_2-MIL-125(Ti), and NH_2-MIL-125(Ti)/TiO_2 (Fig. S3†). The band gap of anatase TiO_2 is 3.2 eV (ref. 15) and TiO_2 has an absorption spectrum in the ultraviolet band ($\lambda < 387$ nm) (Fig. S3† curve a). NH_2-MIL-125(Ti) has two absorption bands at 258 and 371 nm attributed to the $ATA^{2-}Ti^{4+} \rightarrow ATA^{-}Ti^{3+}$ transition within the subunits of the framework.[34] The absorption edge of NH_2-MIL-125(Ti) extended to around 500 nm (Fig. S3† curve b), indicating that NH_2-MIL-125(Ti) could absorb light in the visible region. These results are consistent with previous reports.[19,20] Compared with TiO_2 alone (Fig. S3† curve a), the absorption wavelength of NH_2-MIL-125(Ti)/TiO_2 was broadened largely to the visible region (Fig. S3† curve c), thus NH_2-MIL-125(Ti)/TiO_2 can be used as a photocatalyst in the visible light region.

3.2. Photocurrent behaviors of the prepared electrodes

Fig. 2A shows the photoelectrochemical behaviors of TiO_2/GCE, NH_2-MIL-125(Ti)/TiO_2/GCE, and GOx/CS/NH_2-MIL-125(Ti)/

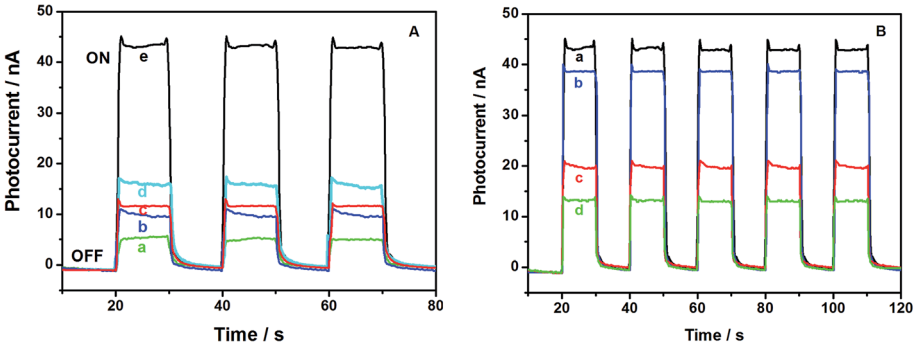

Fig. 2 (A) The photocurrent responses of (a) TiO_2/GCE, (b) NH_2-MIL-125(Ti)/TiO_2/GCE, and (c) GOx/CS/NH_2-MIL-125(Ti)/TiO_2/GCE in a supporting electrolyte of 0.1 M pH 7.0 phosphate buffer; (d) NH_2-MIL-125(Ti)/TiO_2/GCE and (e) GOx/CS/NH_2-MIL-125(Ti)/TiO_2/GCE in the presence of 0.1 M pH 7.0 phosphate buffer containing 0.6 mM glucose; (B) the photocurrent responses of GOx/CS/NH_2-MIL-125(Ti)/TiO_2/GCE in the presence of 0.1 M pH 7.0 phosphate buffer containing 0.6 mM glucose after incubation in (a) 0, (b) 0.1, (c) 1.0, and (d) 10.0 nM acetochlor solution at a bias voltage of 0.2 V and after irradiation with light (λ > 400 nm).

TiO_2/GCE in the absence and presence of 0.6 mM glucose upon light irradiation in 0.1 M pH 7.0 phosphate buffer. Upon photoexcitation with visible light, a series of almost identical PEC responses was obtained. NH_2-MIL-125(Ti)/TiO_2/GCE (Fig. 2A curve b) showed an obviously higher photocurrent response than TiO_2/GCE (Fig. 2A curve a), indicating the improvement of the photocurrent conversion efficiency of TiO_2 upon the addition of NH_2-MIL-125(Ti) because of the strong electronic coupling between the excited-state NH_2-MIL-125(Ti) and the conduction band of TiO_2.[21,31] In comparison with the NH_2-MIL-125(Ti)/TiO_2/GCE electrode, GOx was introduced onto NH_2-MIL-125(Ti)/TiO_2/GCE, and the photocurrent of GOx/CS/NH_2-MIL-125(Ti)/TiO_2/GCE was slightly enhanced (Fig. 2A curve c), possibly owing to the light-harvesting effect of GOx toward visible light as well as the ability of electrons or energy to migrate between GOx and NH_2-MIL-125(Ti)/TiO_2.[35] Further addition of glucose, an enzyme substrate, to the phosphate buffer resulted in a significantly enhanced photocurrent in the GOx/CS/NH_2-MIL-125(Ti)/TiO_2 hybrid system (Fig. 2A curve e). Upon the addition of 0.6 mM glucose, the photocurrent of the GOx/CS/NH_2-MIL-125(Ti)/TiO_2 modified GCE electrode increased by 44 nA, which is 3.5 times the photocurrent increment of 12.6 nA observed in the absence of glucose (Fig. 2A curve c). The reason may be that the immobilized GOx can catalyze the electro-oxidation of glucose into H_2O_2 when this system is exposed to a solution containing glucose. Upon irradiation, the product H_2O_2 acts as a sacrificial electron donor to scavenge the holes in the valence band of the NH_2-MIL-125(Ti)/TiO_2 and improves the efficiency of charge separation, resulting in a prominent photocurrent increase. In a control experiment, slight photocurrent enhancement was observed upon the irradiation of NH_2-MIL-125(Ti)/TiO_2 incubated in glucose without GOx (Fig. 2A curve d). These results further demonstrated that NH_2-MIL-125(Ti)/TiO_2 was an excellent immobilization matrix for GOx, and the adsorbed GOx effectively retained its bioactivity.

Fig. 2B shows that the presence of acetochlor induces the inhibition of GOx. Acetochlor has a high acute toxicity toward GOx and cuts down its enzymatic activity on the substrate (glucose), leading to a decrease in H_2O_2 production. With each increase of the concentration of the added acetochlor, the photocurrent from GOx/CS/NH_2-MIL-125(Ti)/TiO_2/GCE decreased successively. The decrease of the photocurrent is directly proportional to the concentration of the inhibitor in the test solution because the percentage of inhibited enzyme that results after exposure to the inhibitor is quantitatively related to the inhibitor concentration.[36] Owing to the notable change in the PEC signal of the GOx/CS/NH_2-MIL-125(Ti)/TiO_2 hybrid system, the GOx/CS/NH_2-MIL-125(Ti)/TiO_2 functionalized electrode could be used for the PEC biosensing of acetochlor with irradiation with visible light.

3.3. Optimization of GOx/CS/NH_2-MIL-125(Ti)/TiO_2/GCE for acetochlor detection

The experimental variables, including the GOx to NH_2-MIL-125(Ti)/TiO_2 ratio, pH of the supporting electrolyte, inhibition time and concentration of substrate, can affect the detection of acetochlor, and were investigated.

Fig. 3A shows the relationship between the GOx to NH_2-MIL-125(Ti)/TiO_2 ratio and the degree of inhibition of GOx by 0.4 nM acetochlor. This result illustrates that the degree of inhibition attained its maximum when the GOx to NH_2-MIL-125(Ti)/TiO_2 ratio was 10 : 1. Thus, this optimized ratio was chosen for the following experiments.

The bioactivity of the immobilized GOx depends on the pH of the electrolyte. Fig. 3B illustrates the relationship between the pH and the degree of inhibition of GOx by 0.4 nM acetochlor. Considering that the greatest activity of GOx is observed in the pH range 5.5–9.0, being highest at pH 6.5,[37] the influence of the buffer pH on the inhibition response in 0.1 M phosphate buffer in a pH range from 5.5 to 9.0 was studied. It is found that the degree of inhibition of the GOx/CS/NH_2-MIL-125(Ti)/TiO_2 biosensor rises as the pH increases below pH 7.0. When pH value is higher than 7.0, the degree of inhibition drops as the pH increases because the enzyme loses its activity. This is similar to the results reported for GOx immobilized on cobalt or copper hexacyanoferrate[13] and a Au

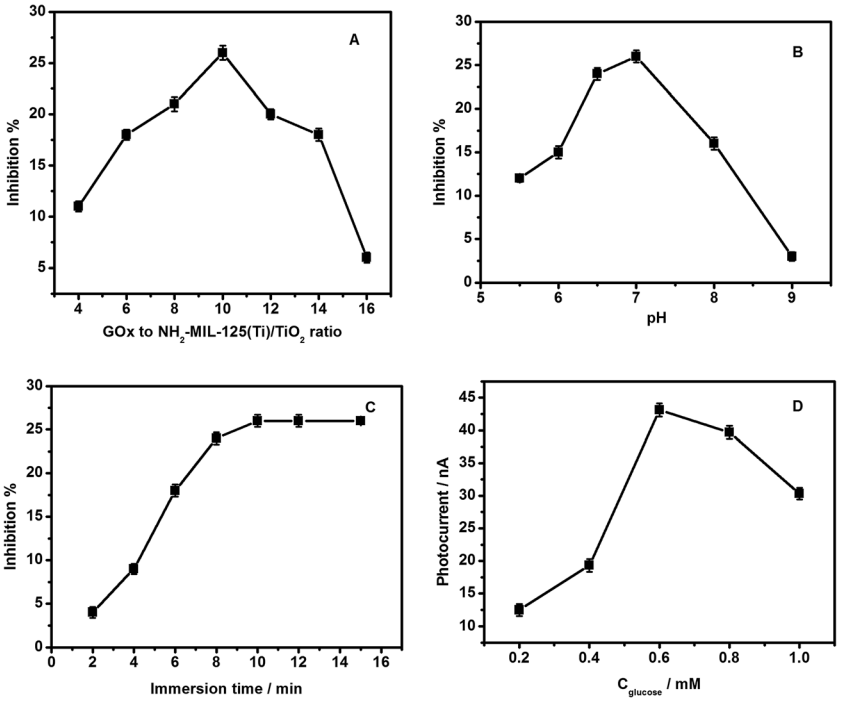

Fig. 3 (A) Influence of the GOx to NH_2-MIL-125(Ti)/TiO_2 ratio on the inhibition of the GOx/CS/NH_2-MIL-125(Ti)/TiO_2 biosensor by 0.4 nM acetochlor in pH 7.0 phosphate buffer; (B) influence of the pH on the inhibition of the GOx/CS/NH_2-MIL-125(Ti)/TiO_2 biosensor by 0.4 nM acetochlor at different pH values; (C) effects of the immersion time in 0.4 nM acetochlor on the inhibition rate; (D) photocurrent value for GOx/CS/NH_2-MIL-125(Ti)/TiO_2 in 0.1 M phosphate buffer after the addition of different concentrations of glucose: 0.2, 0.4, 0.6, 0.8, 1.0 mM (from bottom to top) at a bias voltage of 0.2 V with visible light excitation.

electrode.[38] Therefore pH 7.0 was chosen as the optimum pH for this inhibition study.

The inhibition time is an important factor in pesticide analysis. Fig. 3C shows that the photocurrent from glucose on GOx/CS/NH_2-MIL-125(Ti)/TiO_2/GCE decreased greatly as the immersion time in the acetochlor solution increased from 2 to 10 min and then trended toward a stable value, indicating that the binding interactions with active target groups in the enzyme reached saturation. This tendency for change in the photocurrent reflects an alteration of the enzymatic activity, which in turn results in a change of the interactions with its substrate. Notably, the maximum value of the inhibition by acetochlor was not 100%, which might be attributed to a binding equilibrium between the pesticide and the binding sites in the enzyme.

For an inhibitor biosensor, the concentration of the substrate is another important factor. The effect of glucose concentration on the PEC response of the GOx/CS/NH_2-MIL-125(Ti)/TiO_2 functionalized GCE was investigated (Fig. 3D). The photocurrent increases with the increasing glucose concentration from 0.2 to 0.6 mM, and then goes down upon further increase of the glucose concentration, indicating GOx inhibition by excessive substrate. When the concentration of glucose was too low, the peak current generated by the enzyme electrode was so small that the determination of acetochlor was hardly feasible. However, too high a substrate concentration would cause all the active centers of GOx to be occupied by the substrate and therefore be unable to produce a photocurrent. Therefore, in the present study a glucose concentration of 0.6 mM was chosen for acetochlor determination.

3.4. Analytical performance of the visible-light-activated photoelectrochemical biosensor for acetochlor

Under the optimized experimental conditions, the detection of acetochlor was performed using the GOx/CS/NH_2-MIL-125(Ti)/TiO_2 functionalized electrode. As shown in Fig. 4A, the generated photocurrent decreases with an increase of the acetochlor concentration. The acetochlor inhibition of GOx/CS/NH_2-MIL-125(Ti)/TiO_2/GCE was proportional to its concentration in the ranges from 0.02 to 1.0 nM and 10 to 200 nM. The linearization equations were inhibition (%) = 58.43c (nM) + 3.332 (%), and inhibition (%) = 0.06c (nM) + 69.73 (%), with the correlation coefficients of 0.998 and 0.999, respectively (Fig. 4B). The detection limit was calculated to be about 0.003 nM based on S/N = 3. Table S1† lists the analytical performance of different methods for acetochlor detection. This method is more sensitive than the MSPE-DLLM/GC method,[39] the SPME/GC-MS method[40] and a photocatalytic-electrochemical sensor,[27] but is less sensitive than the UPLC/MS/MS method.[41] However, this value is below the approximate acetochlor concentration required by the USEPA. Therefore, the proposed method is suitable for testing for acetochlor in real samples.

The repeatability of the method was examined at a concentration of 0.80 nM acetochlor with the same electrode, and a relative standard deviation (RSD) of 6.1% was estimated from

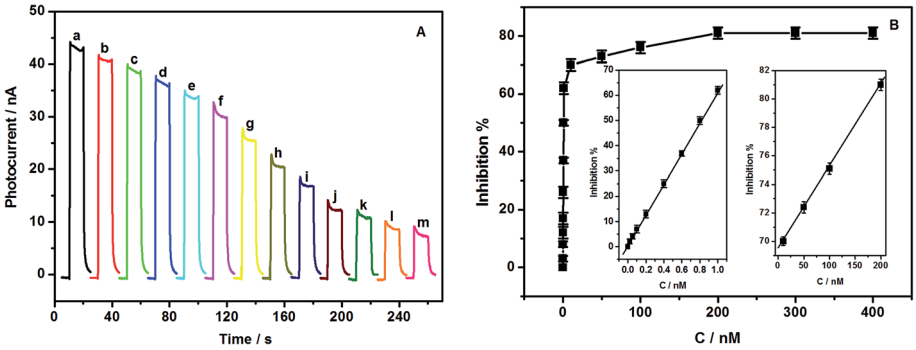

Fig. 4 (A) Photocurrent responses of the GOx/CS/NH_2-MIL-125(Ti)/TiO_2 functionalized electrode toward 0.6 mM glucose under visible light after incubation with 0, 0.02, 0.05, 0.1, 0.2, 0.4, 0.6, 0.8, 1.0, 10, 50, 100 and 200 nM (from a to m) acetochlor solutions. (B) Calibration curves between the acetochlor concentration and efficiency of inhibition of GOx/CS/NH_2-MIL-125(Ti)/TiO_2/GCE. All the results were measured in 0.1 M pH 7.0 phosphate buffer containing 0.6 mM glucose. The bias voltage was 0.2 V with irradiation with a halogen lamp light source ($\lambda > 400$ nm).

fifteen successive assays. To investigate the fabrication reproducibility, a 0.80 nM acetochlor solution was measured by ten biosensors. The RSD of the peak current was 7.5%, revealing excellent reproducibility. The stability of the biosensor could be maintained by storing it at 4 °C in a refrigerator. No obvious decrease in the response to glucose was observed in the first 10 days of storage. After a 30 day storage period, the sensor retained 92.5% of its original photocurrent response.

The interfering compounds that coexist with acetochlor in fruit and vegetable samples were studied to learn the effect of these compounds on the efficiency and selectivity of the proposed analytical method for acetochlor detection. No change in the detection of 0.8 nM acetochlor was found after the addition of 1000-fold concentrations of sucrose, glycine, citric acid, K^+, Na^+, and Ca^{2+}. The addition of 10-fold mass ratios of prometryn, clethodim, cycloxydim, and sethoxydim had no influence on the determination of acetochlor. These results indicated that the biosensor has an excellent selectivity for acetochlor, and it might be applied to monitoring acetochlor in real samples.

3.5. Real sample analysis

The feasibility of the developed biosensors was evaluated by analyzing real fruit and vegetable samples. The samples used for the recovery studies were previously tested by the GC-MS method and proved to be free from acetochlor. We performed the recovery tests by adding different amounts of acetochlor to the samples. The accuracy of the method was also assessed by comparing the electrochemical results with those obtained by GC-MS, and the results are summarized in Table 1. These results implied that the biosensor was capable of practical application.

4. Conclusions

In conclusion, a novel inhibition PEC biosensor for the detection of acetochlor was constructed based on the inhibition of GOx, using newly synthesized NH_2-MIL-125(Ti)/TiO_2 nanocomposites; and the efficient integration of a GOx/CS/NH_2-MIL-125(Ti)/TiO_2 hybrid was accomplished for developing a PEC biosensing platform for the first time. Upon visible light irradiation, the biofunctional GOx/CS/NH_2-MIL-125(Ti)/TiO_2/GCE electrode showed obvious photocurrent changes, which were inhibited by acetochlor. The fabricated biosensor shows many unique advantages such as rapid response, excellent sensitivity, good reproducibility, ideal stability and fine applicability for the detection of acetochlor in real samples. The good performance,

Table 1 Results for the measurement of acetochlor in fruit and vegetable samples ($n = 5$)

Sample	Spiked (nM)	Found (nM)	Recovery (%)	RSD (%)	Found by GC-MS (nM)
Strawberry	0.10	0.095	95.0	4.9	0.097
	0.40	0.406	101.5	2.5	0.381
	0.80	0.782	97.8	2.7	0.783
Tomato	0.20	0.193	96.5	2.7	0.205
	0.40	0.377	94.3	4.6	0.387
	0.80	0.786	98.3	1.7	0.782
Cucumber	0.10	0.102	102.0	2.8	0.097
	0.40	0.384	96.0	3.5	0.381
	0.80	0.758	94.8	2.3	0.762
Greens	0.20	0.195	97.5	3.7	0.193
	0.40	0.383	95.8	4.1	0.405
	0.60	0.623	103.8	2.6	0.589

simple and inexpensive fabrication and ease of use endow the nanostructured biosensor with great potential for practical application.

Acknowledgements

We gratefully acknowledge the financial support from the National Natural Science Foundation of China (No. 21275124, 21275125, and 21575124), the PAPD of Jiangsu Higher Education Institutions, the Qing Lan Project of Jiangsu Province (2014-23, 11KJB150019, 2016-15), The fifth "333 high-level talent Training project" of Jiangsu Province (2016-7), The High-End Talent Project of Yangzhou University, the Scientific and Technological Project of Yangzhou (YZ2015030), the Natural Science Research Projects of Jiangsu Higher Education (16KJB150044), and a Yangzhou Polytechnic Institute school project (2015XK01).

Notes and references

1 California Department of Food and Agriculture, *International Maximum Residue Limits Database [DB/OL]*, 2007, http://www.calagexports.com/mrl_databases.asp.
2 U. S. Environmental Protection Agency (USEPA), *Prevention, Pesticides and Toxic Substances. Questions and Answers, Conditional Registration of Acetochlor*, U. S. EPA, Washington, DC, 1994, p. 18.
3 W. Tan, Q. L. Li and H. Zhai, *Pestic. Biochem. Physiol.*, 2012, **103**, 210–218.
4 W. S. Xiang, X. J. Wang, J. Wang and Q. Wang, *Chin. J. Chromatogr.*, 2002, **20**, 474–475.
5 W. Y. Yu, H. Zhang, W. D. Huang, J. P. Chen and X. M. Liang, *Talanta*, 2005, **65**, 172–178.
6 J. Yakovleva, A. V. Zherdev, V. A. Popova, S. A. Eremin and B. B. Dzantiev, *Anal. Chim. Acta*, 2003, **491**, 1–13.
7 W. W. Tu, J. P. Lei, P. Wang and H. X. Ju, *Chem.–Eur. J.*, 2011, **17**, 9440–9447.
8 Q. Xu, L. J. Cai, H. J. Zhao, J. Q. Tang, Y. Y. Shen, X. Y. Hu and H. B. Zeng, *Biosens. Bioelectron.*, 2014, **63**, 294–300.
9 X. Y. Li, Z. Z. Zheng, X. F. Liu, S. L. Zhao and S. Q. Liu, *Biosens. Bioelectron.*, 2015, **64**, 1–5.
10 H. J. Shi, G. H. Zhao, M. C. Liu and Z. L. Zhu, *Electrochem. Commun.*, 2011, **13**, 1404–1407.
11 Q. L. Huang, H. Chen, L. L. Xu, D. Q. Lu, L. L. Tang, L. T. Jin and Z. A. Xu, *Biosens. Bioelectron.*, 2013, **45**, 292–299.
12 J. G. Ayenimo and S. B. Adeloju, *Talanta*, 2015, **137**, 62–70.
13 M. E. Ghica, R. C. Carvalho, A. Amine and C. M. A. Brett, *Sens. Actuators, B*, 2013, **178**, 270–278.
14 L. Xia, J. Song, R. Xu, D. L. Liu, B. Dong, L. Xu and H. W. Song, *Biosens. Bioelectron.*, 2014, **59**, 350–357.
15 J. X. Qiu, S. Q. Zhang and H. J. Zhao, *Sens. Actuators, B*, 2011, **160**, 875–890.
16 G. L. Wang, J. J. Xu, H. Y. Chen and S. Z. Fu, *Biosens. Bioelectron.*, 2009, **25**, 791–796.
17 M. A. Nasalevich, M. G. Goesten, T. J. Savenije, F. Kapteijn and J. Gascon, *Chem. Commun.*, 2013, **49**, 10575–10577.
18 C. H. Hendon, D. Tiana, M. Fontecave, C. Sanchez, L. D'arras, C. Sassoye, L. Rozes, C. Mellot-Draznieks and A. Walsh, *J. Am. Chem. Soc.*, 2013, **135**, 10942–10945.
19 Y. Horiuchi, T. Toyao, M. Saito, K. Mochizuki, M. Iwata, H. Higashimura, M. Anpo and M. Matsuoka, *J. Phys. Chem. C*, 2012, **116**, 20848–20853.
20 D. R. Sun, L. Ye and Z. H. Li, *Appl. Catal., B*, 2015, **164**, 428–432.
21 P. A. Sant and P. V. Kamat, *Phys. Chem. Chem. Phys.*, 2002, **4**, 198–203.
22 S. Tambwekar, D. Venugopal and M. Subrahmanyam, *Int. J. Hydrogen Energy*, 1999, **24**, 957–963.
23 D. Q. Jin, Q. Xu, L. Y. Yu and X. Y. Hu, *Microchim. Acta*, 2015, **182**, 1885–1892.
24 C. Iamsamai, S. Hannongbua, U. Ruktanonchai, A. Soottitantawat and S. T. Dubas, *Carbon*, 2010, **48**, 25–30.
25 X. H. Kang, J. Wang, H. Wu, I. A. Aksay, J. Liu and Y. H. Lin, *Biosens. Bioelectron.*, 2009, **25**, 901–905.
26 R. Xu, Y. D. Jiang, L. Xia, T. X. Zhang, L. Xu, S. Zhang, D. L. Liu and H. W. Song, *Biosens. Bioelectron.*, 2015, **74**, 411–417.
27 D. Q. Jin, Q. Xu, Y. J. Wang and X. Y. Hu, *Talanta*, 2014, **127**, 169–174.
28 C. Zlotea, D. Phanon, M. Mazaj, D. Heurtaux, V. Guillerm, C. Serre, *et al.*, *Dalton Trans.*, 2011, **40**, 4879–4881.
29 S. K. Kisku and S. K. Swain, *J. Am. Ceram. Soc.*, 2012, **95**, 2753–2757.
30 X. L. Ren, D. Chen, X. W. Meng, F. Q. Tang, X. Q. Hou, D. Han and L. Zhang, *J. Colloid Interface Sci.*, 2009, **334**, 183–187.
31 M. Dan-Hardi, C. Serre, T. Frot, L. Rozes, G. Maurin, C. Sanchez and G. Ferey, *J. Am. Chem. Soc.*, 2009, **131**, 10857.
32 R. W. Liang, L. J. Shen, F. F. Jing, W. M. Wu, N. Qin, R. Lin and L. Wu, *Appl. Catal., B*, 2015, **162**, 245–251.
33 Z. J. Yang, Y. Tang, J. Li, Y. C. Zhang and X. Y. Hu, *Biosens. Bioelectron.*, 2014, **54**, 528–533.
34 H. Khajavi, J. Gascon, J. M. Schins, L. D. A. Siebbeles and F. Kapteijn, *J. Phys. Chem. C*, 2011, **115**, 12487–12493.
35 J. M. Gong, X. Q. Wang, X. Li and K. W. Wang, *Biosens. Bioelectron.*, 2012, **38**, 43–49.
36 A. Amine, H. Mohamed, I. Bourais and G. Palleschi, *Biosens. Bioelectron.*, 2006, **21**, 1405–1423.
37 O. Courjean and N. Mano, *J. Biotechnol.*, 2011, **151**, 122–129.
38 C. Chen, Q. J. Xie, L. H. Wang, C. Qin, F. Y. Xie, S. Z. Yao and J. H. Chen, *Anal. Chem.*, 2011, **83**, 2660–2666.
39 S. S. Bai, Z. Li, X. H. Zang, C. Wang and Z. Chin, *J. Anal. Chem.*, 2013, **41**, 1177–1182.
40 X. Q. Xu, H. H. Yang, L. Wang, B. Han, X. R. Wang and F. S. C. Lee, *Anal. Chim. Acta*, 2007, **591**, 81–96.
41 G. Gervais, S. Brosillon, A. Laplanche and C. Helen, *J. Chromatogr. A*, 2008, **1202**, 163–172.

